

# The dynamical link between surface cyclones, upper-tropospheric Rossby wave breaking and the life cycle of the Scandinavian blocking

C. Michel,<sup>1</sup> G. Rivière,<sup>1</sup> L. Terray,<sup>2</sup> and B. Joly<sup>1</sup>

Received 14 March 2012; revised 17 April 2012; accepted 19 April 2012; published 18 May 2012.

[1] The Scandinavian blocking (SB) is a well-known quasi-stationary state of the atmospheric flow and one of the four main weather regimes over the Euro-Atlantic domain in winter. The aim of our study is to analyze the link between surface cyclones, upper-tropospheric Rossby wave breakings and the life cycle of SB using ERA-40 reanalysis. The onset and decay of SB are studied by considering the preferential transitions from the zonal regime to SB and from SB to the Greenland anticyclone regime. During the SB onset, Atlantic cyclones have straight trajectories that extend toward the north of Scandinavia. These surface cyclones are associated with anticyclonic wave breakings in the upper troposphere over Europe. During the SB decay, cyclones are much less present in the eastern part of the Atlantic and most of them present curved trajectories in mid-Atlantic. They are shown to be linked to cyclonic wave breakings to the south of Greenland. **Citation:** Michel, C., G. Rivière, L. Terray, and B. Joly (2012), The dynamical link between surface cyclones, upper-tropospheric Rossby wave breaking and the life cycle of the Scandinavian blocking, *Geophys. Res. Lett.*, 39, L10806, doi:10.1029/2012GL051682.

## 1. Introduction

[2] The low-frequency atmospheric variability is commonly studied using linear techniques such as the decomposition into Empirical Orthogonal Functions (EOFs) [e.g., Barnston and Livezey, 1987]. The two first EOFs of the geopotential in winter over the North Atlantic are the so-called North Atlantic Oscillation (NAO) and the East Atlantic (EA) pattern. Weather regimes (WRs) correspond to another view of the low-frequency variability which is based on the search of recurrent and persistent atmospheric circulation states and are usually identified using partitioning algorithms [e.g., Michelangeli et al., 1995]. Four main weather regimes are usually found over the North Atlantic: the Atlantic ridge (AR), the Greenland anticyclone (GA), the zonal WR (Z) and the Scandinavian blocking (SB). WRs are closely related to the EOFs patterns since Z mainly corresponds to the positive NAO phase (NAO+), GA to the negative NAO phase (NAO−), AR to the positive EA phase and SB is linked to the third or fourth EOF in the Atlantic

[Cassou et al., 2004]. However, as shown by the previous study, WRs have the advantage of revealing nonlinear effects and spatial asymmetries that cannot appear in the EOF decomposition. The variability of the Atlantic storm-track according to the NAO/EA patterns is rather well-known [e.g., Raible, 2007; Pinto et al., 2009] but its link with WRs much less. The purpose of the present study is to clarify the role of the Atlantic storm-track during a preferential sequence between WRs in which SB is directly involved. It consists of the Z to SB transition followed by the SB to GA transition. This sequence was initially found by Vautard [1990] and is robust as shown by the recent study of Luo et al. [2011] on the last twenty years (1991 to 2009). It is also consistent with previous studies [Crocini-Maspoli et al., 2007; Woollings et al., 2008; Sung et al., 2011] which identified the European or Scandinavian blocking as a precursor of NAO−. In some sense, this sequence reflects the preferential onset and decay stages of SB.

[3] The onset, maintenance and decay of the blocking have been widely studied by numerical [De Pondeca et al., 1998; Li et al., 1999; Jiang and Wang, 2010] and observational [Nakamura et al., 1997; Michelangeli and Vautard, 1998; Altenhoff et al., 2008] approaches. Two kinds of wave precursors to the SB formation have been identified; one is related to the propagation of planetary Rossby wave trains and the other involves the breaking of synoptic-scale waves. The presence of these two precursors has been confirmed recently by Michel and Rivière [2011] in their study of the Z to SB transition. The transition is first triggered by a low-frequency wave train coming from the Atlantic subtropics and then reinforced by synoptic Rossby wave breaking events (RWBs). The SB to GA transition, that is the preferential SB decay phase, is shown to be mainly driven by RWBs and more precisely cyclonic wave breaking events to the south of Greenland [Michel and Rivière, 2011].

[4] Many other studies made the link between surface synoptic-scale transient eddies and the blocking onset, its maintenance and amplification. Colucci [1985] suggested that the interactions between explosive surface cyclogenesis and the planetary-scale flow reinforce the incipient blocks but according to Lupo and Smith [1994], cyclogenesis exhibits an explosive development only in some cases.

[5] The novelty of this paper is to emphasize the link between surface cyclones properties and RWBs characteristics at upper levels during the onset and decay of SB through the study of the two preferred WRs transitions implying SB. More precisely, we want to answer the two following questions: Are there differences in the position and intensity of the surface cyclones between the onset,

<sup>1</sup>CNRM-GAME, Météo-France/CNRS, Toulouse, France.

<sup>2</sup>CERFACS, Toulouse, France.

Corresponding author: C. Michel, CNRM-GAME, Météo-France/CNRS, 42 av. G. Coriolis, F-31057 Toulouse CEDEX 1, France. (clio.michel@meteo.fr)

**Table 1.** Number of Transitions Between the Initial Weather Regime (Line) and the Future Weather Regime (Column). Bold numbers correspond to the transitions studied in this paper

	SB <sup>a</sup>	GA <sup>b</sup>	AR <sup>c</sup>	Z <sup>d</sup>
SB	40	<b>33</b>	18	33
GA	16	47	9	18
AR	23	18	42	36
Z	<b>43</b>	10	35	50

<sup>a</sup>Scandinavian blocking.

<sup>b</sup>Greenland anticyclone.

<sup>c</sup>Atlantic Ridge.

<sup>d</sup>Zonal.

mature and decay stages of SB? How are these differences related to various kinds of upper-tropospheric RWBs?

## 2. Data and Methodology

[6] In the present study, the 40-yr European Centre for Medium-Range Weather Forecasts (ECMWF) Re-Analysis (ERA-40) data set [Uppala *et al.*, 2005] is used. In particular, we use the daily-mean potential vorticity (PV) on the 300, 315, 330 and 350-K isentropic surfaces to detect RWBs [Michel and Rivière, 2011] and the 6-H relative vorticity (RV) on the 850-hPa level to identify cyclogenesis. The data cover the period from 16 October to 15 April for years from 1958 to 2001 corresponding to 43 extended winters.

[7] Each day of this period is associated with one particular WR among the four mentioned in the introduction using the dynamical cluster algorithm developed by Michelangeli *et al.* [1995] and applied to the geopotential at 500 hPa. Therefore, we were able to define transitions between the four WRs. A transition is defined over a period of twelve days with six consecutive days of one regime *a* followed by six consecutive days of another regime *b*. The day of transition, denoted as T, is the first day of the future regime *b*. The duration of the period is chosen so as to be sure that from T-3 day to T + 2 day, the flow is in the transition between the two WRs. These transitions allowed us to study the typical onset (T to T + 2 days for the Z to SB transition) and decay (T-3 to T-1 days for the SB to GA transition) phases of SB. Table 1 shows the number of transitions between the different WRs. The most probable successor to a given WR is itself confirming the persistence of WRs. The most probable successor to Z distinct from itself is SB. There are two most probable successors to SB which are GA and Z but we have checked that GA is the most robust one by defining transitions in other ways [see, e.g., Michel and Rivière, 2011]. It confirms the preferential transitions mentioned in the introduction.

[8] An automatic detection algorithm of RWBs is used here that systematically identifies large-scale and irreversible overturnings of the PV gradient on an isentropic surface. To distinguish between cyclonic and anticyclonic wave breaking events (CWBs and AWBs), that occur respectively at the end of the two distinct baroclinic wave life cycles LC1 and LC2 [Thorncroft *et al.*, 1993], geometrical considerations on the PV-isolines are made (see Rivière [2009] and Michel and Rivière [2011] for more details). The frequencies of occurrence of AWBs and CWBs are then performed by averaging over time and over the four isentropic levels to cover all the tropopause from the equator to the North Pole.

[9] The tracking algorithm of Ayrault and Joly [2000] is used to get surface cyclone statistics. It is based on the detection and tracking of RV maxima at 850 hPa with a 6-hourly time step. Since distinct tracking algorithms may lead to different results [Raible *et al.*, 2008], a summary of the algorithm is provided in the auxiliary material as well as a cyclone climatology (see Figure S1) to be compared with previous studies [e.g., Hoskins and Hodges, 2002; Ulbrich *et al.*, 2009].<sup>1</sup> In the present study, we only retained systems whose RV is greater or equal to  $2 \cdot 10^{-4} \text{ s}^{-1}$  to avoid the detection of relatively weak systems. Their frequency of occurrence is of the order of 3 to 4 per week in the Atlantic. It has been checked that taking a lower threshold ( $10^{-4} \text{ s}^{-1}$ ) gives quite similar results while considering no threshold at all does not. Tracks densities are averaged over the three days of the onset and decay stages of SB and expressed as number of cyclones per day of transition. They are compared to the track density averaged over all the days of SB. The mean intensity of the cyclone, that is the maximum of RV along the trajectory, during the different stages of SB is computed as well.

## 3. Results

[10] The track density for all the days of SB (Figure 1a) exhibits large values over the east coast of North America, between Greenland and Iceland and north of Scandinavia. The track density is closely related to the typical position of the mid-latitude jet during SB. By subtracting the cyclone track density of the blocking (Figure 1a) to the cyclone track densities of the two stages of SB, the preferred paths during the onset and decay of SB are highlighted. During the onset stage (Figure 1b), cyclones are significantly more frequent over a large region to the east of 40°W from Southeastern Greenland to the north of Scandinavia than when the regime is well established. During the SB decay (Figure 1c), the cyclones are less frequent in these regions, but are more frequent in the mid-Atlantic around 20°W,40°N. These preferred paths can also be seen by plotting trajectories of the cyclones which stay at least one complete day during the onset (decay) period of the Z to SB (SB to GA) transition in a large domain encompassing the North Atlantic ocean (90°W–40°E,30°N–85°N). For the Z to SB (SB to GA) transition, there are 83 (55) trajectories. Tracks colors on Figures 1d and 1e are determined as follows. Blue trajectories refer to those located between Greenland and Iceland at their extreme end. Light blue trajectories are those reaching the western side of Greenland, purple those reaching the north of Scandinavia and orange ones those reaching Europe or a latitude lower than 40°N. During the SB onset, there are many more trajectories to the north of Scandinavia than during its decay while in the rest of the Atlantic differences are less obvious (compare Figures 1d and 1e). Trajectories close to the point 30°W,50°N (mainly the blue ones) feature a strong curvature from the east coast of North America to the southeast of Greenland. They are present for both stages of SB but correspond to the most populated category during the SB decay and are more present near 20°W,40°N (see the positive anomaly of density at this location on Figure 1c). Note also that some of them are so much curved during the

<sup>1</sup>Auxiliary materials are available in the HTML. doi:10.1029/2012GL051682.

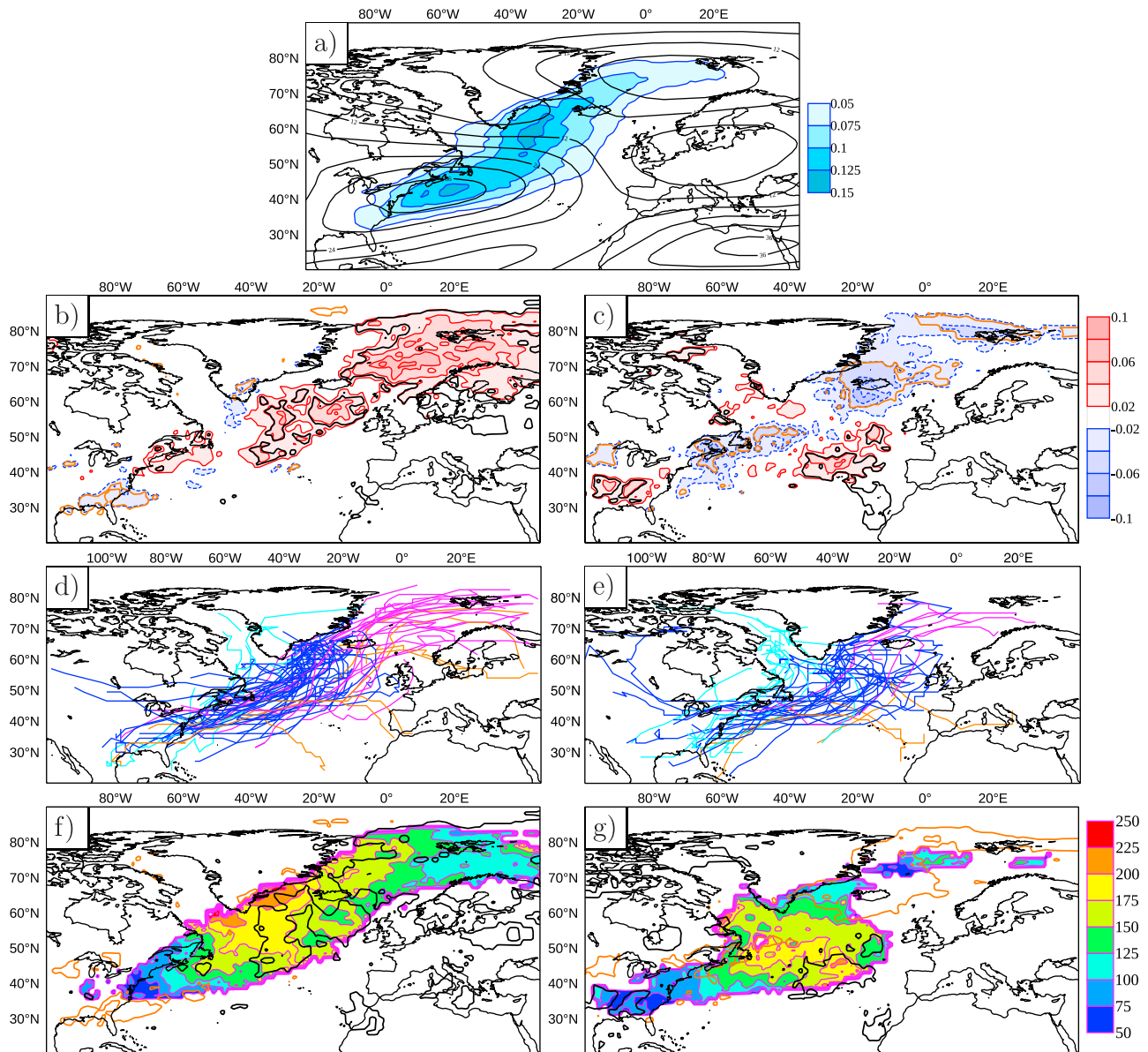


**Figure 1.** (a) Cyclone track density for blocking days (shading, unit is  $\text{day}^{-1}$ ) and the 300-hPa zonal wind (black contours; first contour and interval are  $6 \text{ m s}^{-1}$ ). Left (right) column refers to the onset (decay) of SB. (b, c) Difference between the cyclone track densities for SB onset and decay and the cyclone track density for blocking days plotted in Figure 1a. (d, e) Storm trajectories (colors are explained in section 3). (f, g) Mean intensity (shading, unit is  $10^{-6} \text{ s}^{-1}$ ). In Figures 1b, 1c, 1f, and 1g, black and orange contours show zones that exceed the 90% confidence level in absolute value calculated with a bootstrapping method.

decay stage that they correspond to a northwestward motion of the cyclones before reaching Greenland. Figures 1f and 1g present the mean cyclone intensity for the two phases. During the onset, the cyclones have relatively high intensities with an averaged  $\text{RV} \geq 1.5 \cdot 10^{-4} \text{ s}^{-1}$  in the region between Greenland, Iceland and England (Figure 1f). To the north of Scandinavia, cyclones are fewer and they do not have very high values especially around  $20^\circ\text{E}, 75^\circ\text{N}$  where they only reach values less than  $1.25 \cdot 10^{-4} \text{ s}^{-1}$ . However, these values are significantly higher than those reached during a normal day of SB (see black contours for the statistical significance). On the contrary, when the blocking is decaying, cyclones attain large amplitudes in the mid-

Atlantic far from the Greenland area and very close to the region where they are deflected northward (Figure 1g).

[11] Let us now make the link between this behavior at the surface and RWBs in the upper troposphere. As the blocking appears, AWBs become more frequent over Europe and CWBs between the south of Greenland and Iceland as shown in Figure 2a. The low-frequency zonal wind tendency, due to the sum of the nonlinear high-frequency (periods < 10 days) and low-frequency (periods > 10 days) eddy vorticity fluxes, reflects the impact of these distinct RWBs. In the eastern Atlantic, this term induces deceleration of the zonal wind over Europe in the AWB area and acceleration at  $70^\circ\text{N}$  showing the reinforcement of the Scandinavian high by

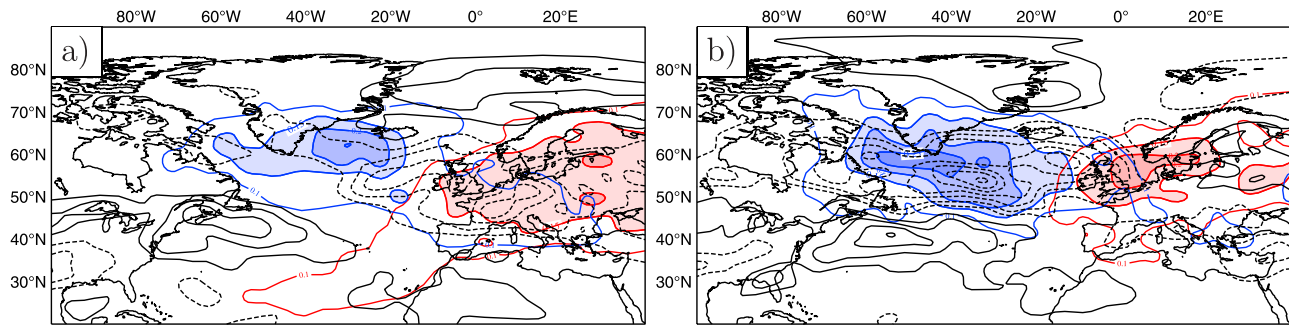


**Figure 2.** CWB and AWB frequencies averaged over the four isentropic levels (blue and red shading respectively, first contour is  $0.1 \text{ day}^{-1}$  and interval is  $0.05 \text{ day}^{-1}$ ) and the zonal wind tendency due to the nonlinear eddy vorticity fluxes at 300 hPa (black contours, interval is  $2 \cdot 10^{-5} \text{ m s}^{-2}$ , the zero contour is omitted and solid (dashed) lines refer to positive (negative) values) for the SB (a) onset and (b) decay.

AWBs. In the western Atlantic, the presence of CWBs implies a deceleration area south of Greenland and an acceleration around  $40^\circ\text{N}$  but the tendencies are weaker and less important for the blocking itself. The greater cyclone activity east of Iceland (see Figure 1b or purple trajectories of Figure 1d) should be linked with AWBs as the cyclones advect low PV from the south of Greenland to the north of Scandinavia and participate in the PV gradient reversal at upper levels. During the SB decay, CWBs are much more frequent, their density covers a much larger area while the AWBs density covers a smaller area localized over England (Figure 2b). This dominance of CWBs at this stage is also revealed by the nonlinear tendency term which exhibits a zone of zonal wind deceleration in the CWB area at  $30^\circ\text{W}, 50^\circ\text{N}$  and a zone of acceleration more to the south. These events trigger the appearance of GA. It is consistent with the large amplitudes reached by the surface cyclones at  $30^\circ\text{W}, 45^\circ\text{N}$  (Figure 1g) and the curved trajectories (Figure 1e). Indeed, the northwestward motion of these cyclones toward Greenland allows low PV advection there and the formation of GA.

[12] Two examples illustrate these two transitions (Figure 3). During the SB onset on Figures 3a–3c, a surface cyclone first interacts with an upper PV streamer, then moves northeastward and advects low-PV air toward north of Scandinavia in connection with an AWB over Eastern Europe. During the SB decay on Figures 3d–3f, a surface cyclone is formed over North America. Its eastward motion is accompanied by an eastward motion of high-PV air at upper levels and the advection of low-PV air toward Greenland, especially during its decay stage in mid-Atlantic. This illustrates the usual CWB event that is responsible for the SB decay.

#### 4. Discussion and Conclusions

[13] In the present study, the preferential sequences between WRs from Z to SB and from SB to GA serve as a framework to analyze the most probable onset and decay stages of SB using ERA-40 data set. It is shown that surface cyclones differ much more in position than in intensity between these two stages and that these differences are closely connected to distinct upper-tropospheric RWBs. During the SB onset, cyclones have straight northeastward oriented trajectories that extend from North America toward

the north of Scandinavia with a strong intensity near Greenland whereas during the SB decay, cyclones reach Greenland with curved trajectories over the mid-Atlantic in a region where they reach their maximum of intensity. During the SB onset, cyclones slightly wrap the low-PV air around them but since they are mainly shifted northeastward by the background flow, they advect the low-PV air northeastward as well causing an AWB over Europe. In contrast, during the SB decay, cyclones succeed on a sustained wrapping of low-PV air around them that advects the low-PV air northwestward and causes a CWB on its northern flank favouring the appearance of GA.

[14] Two questions can be raised from the previous study. How can we explain these distinct behaviors of synoptic eddies during the two transitions? Can it be useful to understand why they correspond to a preferential sequence between WRs?

[15] In the Z to SB transition, the background flow is straight and northeastward oriented (not shown). It advects the cyclones rapidly northeastward, prevents the occurrence of a sustained CWB around Greenland and favors the formation of AWB more downstream that reinforces SB. In contrast, prior to the SB to GA transition, the flow is more curved and presents a rapid poleward deflection to the southeast of Greenland. In such a case, the cyclones are advected until reaching this deflection area that acts as a barrier for the downstream motion of the cyclones. They stay long enough in this region to cause a sustained CWB event. Furthermore, this CWB event is much more likely to occur in the second case because it is much easier for a cyclone to reverse the PV gradient when the PV isolines are almost south-north oriented than when they are southwest-northeast oriented as in the first case. The key role played by the background flow characteristics upstream of the Scandinavian high has been confirmed by comparing the low-frequency PV isolines for the different decay stages of SB (SB to GA, SB to AR and SB to Z) (see Figure S2 in the auxiliary material). PV isolines are almost aligned with the meridians in the SB to GA transition three days before the transition while they are more southwest-northeast tilted before the other two transitions. It confirms that the CWB event is more favored when the poleward deflection of the background flow is more abrupt. Furthermore, it may explain why the SB to GA transition is more likely to occur because this deflection area is more and more present when

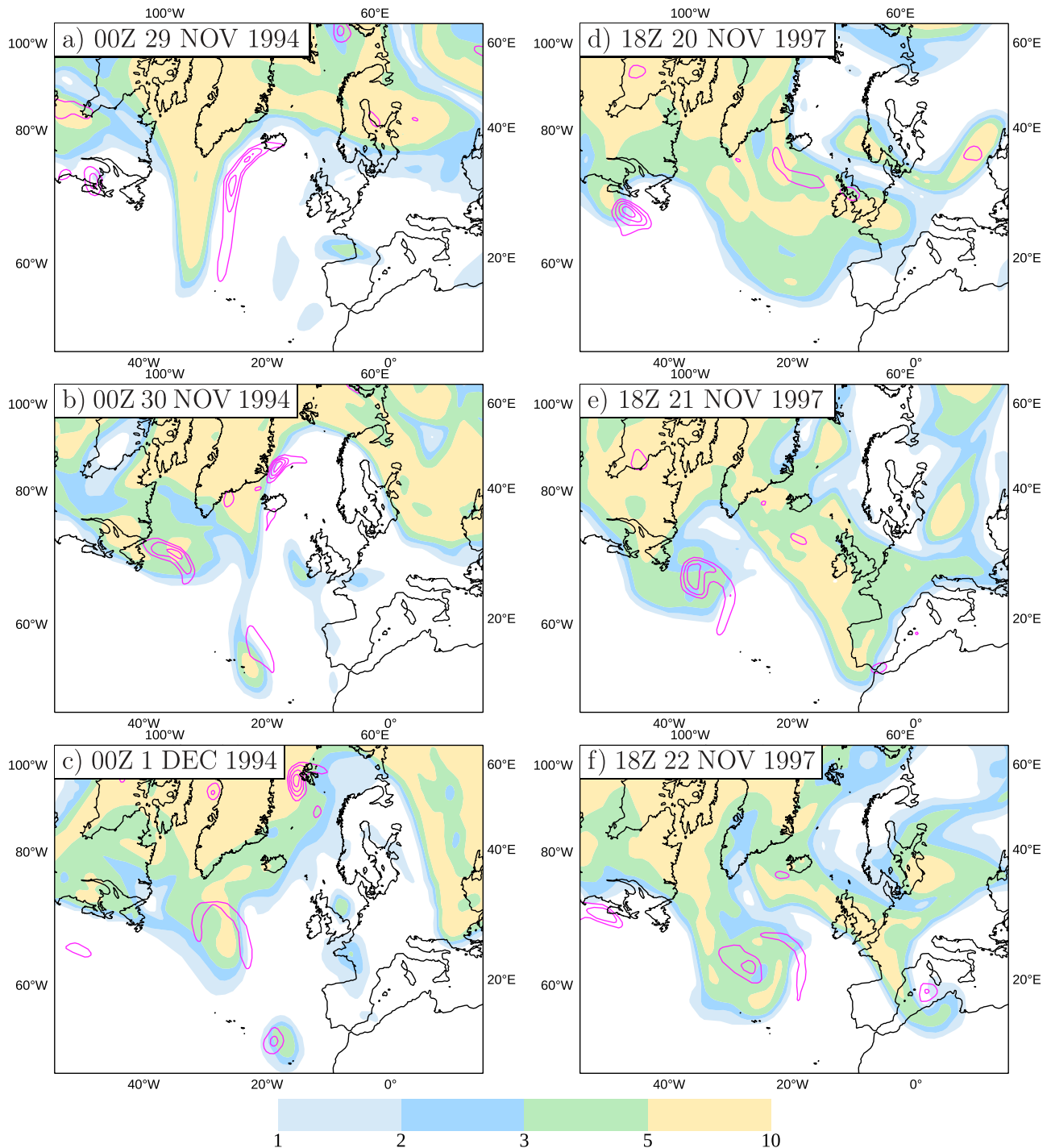


**Figure 3.** Relative vorticity at the 850-hPa level (purple contours: first contour is  $10^{-4} \text{ s}^{-1}$  and interval is  $5 \cdot 10^{-5} \text{ s}^{-1}$ ) and PV at the 315-K level (shading, units: PVU) for two particular weather regime transitions. (a–c) T-5 to T-3 days of the Z to SB transition (T = 26 nov 1994) and (d–f) T + 3 to T + 5 days of the SB to GA transition (T = 25 nov 1997).

the Scandinavian high and the more upstream low are reinforced during the SB regime. In other words, the present study supports the idea that SB contains itself a precursor for its decay which is the deflection area. This constitutes a nonlinear interpretation of the retrograde displacement of wavenumber 1 [Michelangeli and Vautard, 1998]. Of course, it does not say that the SB is not a long-lived WR because there are others elements that make the SB persistent. Concerning the other preferential transition (Z to SB),

its explanation should be more complicated. As shown in Michel and Rivière [2011], it requires the occurrence of a low-frequency wave train triggered by anomalous tropical convection that slightly builds the Scandinavian high first which is then reinforced by the AWB event. It is not clear how this wave train is connected to the Z regime. Further studies should investigate this aspect in connection with the Madden-Julian Oscillation [Cassou, 2008].

[16] **Acknowledgments.** This work has been funded by a CNRS/INSU/LEFE/IDAO project called EPIGONE.

[17] The Editor thanks Joaquim Pinto and Michel dos Santos Mesquita for assisting with the evaluation of this paper.

## References

- Altenhoff, A. M., O. Martius, M. Croci-Maspoli, C. Schwierz, and H. C. Davies (2008), Linkage of atmospheric blocks and synoptic-scale Rossby waves: A climatological analysis, *Tellus, Ser. A*, *60*, 1053–1063.
- Ayrault, F., and A. Joly (2000), The genesis of mid-latitude cyclones over the Atlantic ocean: A new climatological perspective, *C. R. Acad. Sci. Paris Earth Planet. Sci.*, *330*, 173–178.
- Barnston, A. G., and R. E. Livezey (1987), Classification, seasonality and persistence of low-frequency atmospheric circulation patterns, *Mon. Weather Rev.*, *115*, 1083–1126.
- Cassou, C. (2008), Intraseasonal interaction between the Madden-Julian Oscillation and the North Atlantic Oscillation, *Nature*, *455*, 523–527.
- Cassou, C., L. Terray, J. W. Hurrell, and C. Deser (2004), North Atlantic winter climate regimes: Spatial asymmetry, stationarity with time, and oceanic forcing, *J. Clim.*, *17*, 1055–1068.
- Colucci, S. J. (1985), Explosive cyclogenesis and large-scale circulation changes: Implications for atmospheric blocking, *J. Atmos. Sci.*, *42*, 2701–2717.
- Croci-Maspoli, M., C. Schwierz, and H. C. Davies (2007), Atmospheric blocking: Space-time links to the NAO and PNA, *Clim. Dyn.*, *29*, 713–725.
- De Pondaca, M. S. F. V., A. Barçilon, and X. Zou (1998), The role of wave breaking, linear instability, and PV transports in model block onset, *J. Atmos. Sci.*, *55*, 2852–2873.
- Hoskins, B. J., and K. I. Hodges (2002), New perspectives on the Northern Hemisphere winter storm tracks, *J. Atmos. Sci.*, *59*, 1041–1061.
- Jiang, Z., and D. Wang (2010), A study on precursors to blocking anomalies in climatological flows by using conditional nonlinear optimal perturbations, *Q. J. R. Meteorol. Soc.*, *136*, 1170–1180.
- Li, Z., A. Barçilon, and I. M. Navon (1999), Study of block onset using sensitivity perturbations in climatological flows, *Mon. Weather Rev.*, *127*, 879–900.
- Luo, D., Y. Diao, and S. B. Feldstein (2011), The variability of the Atlantic storm track and the North Atlantic Oscillation: A link between intraseasonal and interannual variability, *J. Atmos. Sci.*, *68*, 577–601.
- Lupo, A. R., and P. J. Smith (1994), Climatological features of blocking anticyclones in the Northern Hemisphere, *Tellus, Ser. A*, *47*, 439–456.
- Michel, C., and G. Rivière (2011), The link between Rossby wave breakings and weather regime transitions, *J. Atmos. Sci.*, *68*, 1730–1748.
- Michelangeli, P.-A., and R. Vautard (1998), The dynamics of Euro-Atlantic blocking onsets, *Q. J. R. Meteorol. Soc.*, *124*, 1045–1070.
- Michelangeli, P.-A., R. Vautard, and B. Legras (1995), Weather regimes: Recurrence and quasi stationarity, *J. Atmos. Sci.*, *52*, 1237–1256.
- Nakamura, H., M. Nakamura, and J. L. Anderson (1997), The role of high- and low-frequency dynamics in blocking formation, *Mon. Weather Rev.*, *125*, 2074–2093.
- Pinto, J. G., S. Zacharias, A. H. Fink, G. C. Leckebusch, and U. Ulbrich (2009), Factors contributing to the development of extreme North Atlantic cyclones and their relationship with the NAO, *Clim. Dyn.*, *32*, 711–737.
- Raible, C. C. (2007), On the relation between extremes of midlatitude cyclones and the atmospheric circulation using ERA40, *Geophys. Res. Lett.*, *34*, L07703, doi:10.1029/2006GL029084.
- Raible, C. C., P. M. Della-Marta, C. Schwierz, H. Wernli, and R. Blender (2008), Northern Hemisphere extratropical cyclones: A comparison of detection and tracking algorithm methods and different reanalyses, *Mon. Weather Rev.*, *136*, 880–897.
- Rivière, G. (2009), Effect of latitudinal variations in low-level baroclinicity on eddy life cycles and upper-tropospheric wave-breaking processes, *J. Atmos. Sci.*, *66*, 1569–1592.
- Sung, M.-K., G.-H. Lim, J.-S. Kug, and S.-I. An (2011), A linkage between the North Atlantic Oscillation and its downstream development due to the existence of a blocking ridge, *J. Geophys. Res.*, *116*, D11107, doi:10.1029/2010JD015006.
- Thorncroft, C. D., B. J. Hoskins, and M. E. McIntyre (1993), Two paradigms of baroclinic-wave life-cycle behaviour, *Q. J. R. Meteorol. Soc.*, *119*, 17–55.
- Ulbrich, U., G. C. Leckebusch, and J. G. Pinto (2009), Extra-tropical cyclones in the present and future climate: A review, *Theor. Appl. Climatol.*, *96*, 117–131.
- Uppala, S. M., et al. (2005), The ERA-40 re-analysis, *Q. J. R. Meteorol. Soc.*, *131*, 2961–3012.
- Vautard, R. (1990), Multiple weather regimes over the North Atlantic: Analysis of precursors and successors, *Mon. Weather Rev.*, *118*, 2056–2081.
- Woollings, T., B. Hoskins, M. Blackburn, and P. Berrisford (2008), A new Rossby wave-breaking interpretation of the North Atlantic Oscillation, *J. Atmos. Sci.*, *65*, 609–626.